Inorg. Chem. **2006**, *45*, 3067–3073

Calcium Tetraboride—Does It Exist? Synthesis and Properties of a Carbon-Doped Calcium Tetraboride That Is Isotypic with the Known Rare Earth Tetraborides

Ruth Schmitt, Björn Blaschkowski, Klaus Eichele, and H.-Jürgen Meyer*

Institut für Anorganische Chemie, Universität Tübingen, Auf der Morgenstelle 18, D-72076 Tübingen, Germany

Received October 25, 2005

Crystalline samples of carbon-doped CaB_4 were synthesized by solid-state reactions in sealed niobium ampules from the elements Ca, B, and C. The structure was determined by single-crystal X-ray diffraction (*P*4/*mbm*, $Z = 4$, $a = 7.0989(7)$ Å, $c = 4.1353(5)$ Å, R1 = 0.026, and wR2 = 0.058) revealing an atom arrangement containing a three-dimensional boron network built up from B_6 octahedra and B_2 dumbbells which is well-known from the structures of rare earth tetraborides. Crystals of $CaB_{4-x}C_x$ are black with a metallic luster and behave stable against mineral acids. Band structure calculations indicate that CaB_4 is a stable semiconducting compound with a narrow band gap and that carbon should not necessarily be required for the stability of this compound. The presence of carbon in the crystalline samples of $CaB_{4-x}C_x$ was indicated by electron energy loss spectroscopy, but the carbon content in the samples was estimated to be less than 5% according to inductively coupled plasma–atomic emission spectrometry measurements. The distribution of boron and carbon atoms in the structure was investigated by means of ^{11}B and ^{13}C solid-state magic angle spinning NMR. Measurements of the magnetic susceptibility indicate a temperature-independent paramagnetism down to 20 K.

Introduction

The hexaborides MB_6 of the alkaline earth elements (M = Ca, Sr, and Ba) and most of the rare earth elements (M = Y, La−Er, Yb) are known and well-characterized.[1] They crystallize in a simple cubic structure with the space group $Pm\bar{3}m$, and their structures can be derived from the CsCl structure, by replacing chloride with a B_6 octahedron and cesium with a respective metal atom. Each boron octahedron in the structure is interconnected via apexes by covalent B−B bonds with six adjacent clusters to form a three-dimensional network. In this network structure, the B−B distances between octahedral clusters are shorter than those within the clusters.

Trivalent hexaborides of the rare earth elements exhibit interesting physical properties and applications. One striking example is the application of LaB_6 as a cathode material in electron microscopy, as a result of its good thermoionic emission properties.[2] These hexaborides are metallic compounds because only two electrons are necessary for the saturation of the boron network as $[B_6]^{2-}$, and the surplus electron accounts for the metallic conductivity.[3−6]

Divalent hexaborides (CaB_6, SrB_6, and EuB_6), on the other hand, are considered to be small-gap semiconductors,[7] or rather as semimetals, because of the overlap of an almost-filled band with an almost-empty band near the X point at the Fermi level.[8] High-temperature ferromagnetism once reported for the lanthanum-doped calcium hexaboride $Ca_{1-x}La_xB_6$[9] turned out not to be an intrinsic property of this material. Otani and Mori demonstrated that this effect resulted from iron impurities in the samples.[10]

* Author to whom correspondence should be addressed. E-mail: juergen.meyer@uni-tuebingen.de.

(1) Zuckerman, J. J.; Hagen, A. P. *Inorganic Reactions and Methods*; VCH Weinheim: Weinheim, Germany; Vol. 13, p 84.
(2) Lafferty, J. M. *J. Appl. Phys.* **1951**, *22*, 299−309.
(3) Walch, P. F.; Ellis, D. E.; Mueller, F. M. *Phys. Rev. B* **1977**, *15*, 1859−1866.
(4) Kubo, Y.; Asano, S. *Phys. Rev. B* **1989**, *39*, 8822−8831.
(5) Booth, C. H.; Sarrao, J. L.; Hundley, M. F.; Cornelius, A. L.; Kwei, G. H.; Bianchi, A.; Fisk, Z.; Lawrence, J. M. *Phys. Rev. B* **2001**, *63*, 224302/1−224302/8.
(6) Monnier, R.; Delley, B. *Phys. Rev. B* **2004**, *70*, 193403/1−193403/4.
(7) Longuet Higgins, H. C.; Roberts, M. d. V. *Proc. R. Soc. London, Ser. A* **1954**, *224*, 336−347.
(8) Massidda, S.; Continenza, A.; de Pascale, T. M.; Monnier, R. *Z. Phys. B: Condens. Matter* **1997**, *102*, 83−89.
(9) Young, D. P.; Hall, D.; Torelli, M. E.; Fisk, Z.; Sarrao, J. L.; Thompson, J. D.; Ott, H.-R.; Oseroff, S. B.; Goodrich, R. G.; Zysler, R. *Nature* **1999**, *397*, 412−414.
(10) Otani, S.; Mori, T. *J. Phys. Soc. Jpn.* **2002**, *71*, 1791−1792.

10.1021/ic0518430 CCC: $33.50
Published on Web 03/09/2006

The related alkali carbaborides MB_5C (M = Na and K) form structures that are isotypic with the hexaborides, however, with $^1/_6$ of the boron atoms substituted by a carbon atom.[11,12] Electron counting leads to 20 electrons for both $[B_5C]^-$ in MB_5C and $[B_6]^{2-}$ in CaB_6.

The tetraborides MB_4 are prominent for trivalent rare earth elements and crystallize with the ThB_4-type structure.[13−15] Most of the rare earth tetraborides (M = Nd, Sm, Gd, Tb, Dy, and Ho) show antiferromagnetic behavior, while ErB_4 and YbB_4 are metamagnetic. PrB_4 is the only ferromagnetic tetraboride.[16] LaB_4 seems to have very similar electron emitter qualities to those of LaB_6.[17]

Tetraborides of Sr, Ba, and Eu are unknown. Only a vague indication was given for the existence of CaB_4.[18] Here, we present the carbon-doped tetraboride $CaB_{4-x}C_x$ as the first example of an alkaline earth boride with a ThB_4-type structure.

Experimental Section

Synthesis. All manipulations for the synthesis of $CaB_{4-x}C_x$ were performed in an Ar-filled glovebox (MBraun) with Ca (Strem, 99.99%, dendritic), β-rhombohedral boron (ABCR, crystalline powder, 99.7%), graphite (Strem, carbon 5N), amorphous ^{13}C (Chemotrade, 99%), and B_4C (Riedel-de Haën, X-ray pure) as starting materials.

$CaB_{4-x}C_x$ was first obtained from reactions of Ca, B, and C in 3:2:1 molar ratios in niobium containers. Graphite and boron powders were thoroughly mixed in an agate mortar and then transferred to a niobium container together with chunks of Ca metal. The niobium container was sealed under Ar with an electric arc and then sealed in an evacuated silica ampule. The samples, as protected by two ampules, were heated to 1000 °C in a resistance-heated box furnace (Carbolite) within 2 h and remained at this temperature for 60 h. After cooling the furnace by its natural cooling rate and opening the protecting containers, a black crystalline material embedded into a matrix of excess Ca was obtained. This material was isolated by washing the raw product in diluted hydrochloric acid (pH 3−4). In this step, moisture-sensitive byproducts were also removed that were possibly CaC_2 and CaB_2C_2, which were detected as intermediates in the reaction at 800 °C. In the as-obtained material, small crystals (which later turned out to be $CaB_{4-x}C_x$) were selected under a microscope for a single-crystal X-ray diffraction (XRD) analysis.

All attempts to prepare carbon-free samples from direct combinations of Ca and B with different molar ratios, at reaction temperatures between 800 and 1200 °C, and with different reaction durations yielded exclusively CaB_6. Without the employment of carbon in reactions, we found no trace of a calcium tetraboride phase. After carbon was added to the reaction mixture, the calcium tetraboride phase was always formed.

Our preparative explorations revealed that calcium tetraboride is formed with a small amount of carbon and that yields can be increased in the presence of an excess of calcium (minimum Ca/B ratio of about 3:2). The best results were obtained when the molar ratios of Ca/B/C were 3:2:1.

To explore another starting material, Ca was reacted with B_4C in a 3:1 molar ratio in tantalum tubes. All preparative handling and the treatment after reaction were performed as before. The reaction was carried out at 950 °C for 72 h. After cooling the reaction down, $CaB_{4-x}C_x$ was obtained as the only product detectable in the X-ray powder pattern.

To study the role of carbon in this reaction in more detail, a mixture of Ca and B_4C was heated only at 800 °C and remained at this temperature for 3 days. The powder XRD pattern of the product revealed a mixture of β-rhombohedral boron,[19] CaB_2C_2,[20] and three different modifications of calcium carbide. The relative intensities of the strongest reflections in the XRD powder pattern of tetragonal CaC_2(I),[21] CaB_2C_2, monoclinic CaC_2(II),[21] and monoclinic CaC_2(III)[22] corresponded to an approximate 4:2:2:1 ratio. This mixture was converted into $CaB_{4-x}C_x$ in a following heating procedure at 950 °C for 3 days.

Our various experiments also revealed that a higher reaction temperature tends to produce calcium hexaboride. In this context, our experiments also revealed that $CaB_{4-x}C_x$ is gradually converted into CaB_6 (or possibly $CaB_{6-x}C_x$) at temperatures around 1000 °C in an open vessel under Ar.

X-ray Diffraction Studies. After being washed and dried, the reaction products were ground and inspected with an X-ray powder diffractometer (Stoe, StadIP, Darmstadt) using monochromatic Cu $K_{\alpha1}$ radiation. The powder XRD pattern of the product synthesized from Ca and B_4C (Figure 1) was indexed with the aid of the program system WinXPow (Stoe, Darmstadt),[23] and the lattice parameters were refined using a tetragonal primitive indexing scheme, yielding $a = 7.0625(6)$ Å and $c = 4.1207(4)$ Å (based on 39 reflections).

A single crystal of $CaB_{4-x}C_x$ prepared from Ca, B, and C was selected and mounted in a glass capillary for an intensity measurement with a single-crystal X-ray diffractometer (Stoe, IPDS, Darmstadt). The structure solution and refinement were obtained with the program package SHELX-97[24] in the space group *P*4/*mbm*. The structure refinement was performed with calcium and boron atoms, leading to three distinct boron positions in the crystal structure of CaB_4. After the anisotropic crystal structure refinement of CaB_4, the occupation factors of all boron atoms were refined, but they did not deviate from full occupancies within their standard deviations. Attempts to refine the site occupation factors with boron and carbon on the same position did not lead to reliable results, no matter if one or all three sites were considered. Selected data of the crystal and conditions of the data collection are given in Table 1; atomic positions and isotropic displacement parameters are provided in Table 2; anisotropic displacement parameters are listed in Table 3. Important interatomic distances are given in Table 4.

Analyses. All preparative results pointed out that the presence of carbon is essential for the formation of calcium tetraboride. However, the structure refinement did not give a clue on the presence or distribution of carbon atoms in the structure. GdB_4 as well as other rare earth tetraborides are reported to exist as pure borides. When GdB_4 was crystallized from the Gd−B−C system,

(11) Albert, B.; Schmitt, K. *Chem. Commun*. **1998**, *23*, 2373−2374.
(12) Albert, B.; Schmitt, K. *Chem. Mater*. **1999**, *21*, 3406−3409.
(13) Zalkin, A.; Templeton, D. H. *Acta Crystallogr*. **1953**, *6*, 269−272.
(14) Felten, E. J.; Bender, I.; Post, B. *J. Am. Chem. Soc*. **1958**, *80*, 3479.
(15) Will, G.; Schaefer, W. *J. Less-Common Met*. **1979**, *67*, 31−39.
(16) Buschow, K. H. J.; Creyghton, J. H. N. *J. Chem. Phys*. **1972**, *57*, 3910−3914.
(17) Deacon, J. A.; Hiscocks, S. E. R. *J. Mater. Sci*. **1971**, *6*, 309−312.
(18) Johnson, R. W.; Daane, A. H. *J. Chem. Phys*. **1961**, *65*, 909−915.
(19) Callmer, B. *Acta Crystallogr., Sect. B* **1977**, *33*, 1951−1954.
(20) Albert, B.; Schmitt, K. *Inorg. Chem*. **1999**, *38*, 6159−6163.
(21) Reckeweg, O.; Baumann, A.; Mayer, H. A.; Glaser, J.; Meyer, H.-J. *Z. Anorg. Allg. Chem*. **1999**, *625*, 1686−1692.
(22) Glaser, J.; Dill, S.; Marzini, M.; Mayer, H. A.; Meyer, H.-J. *Z. Anorg. Allg. Chem*. **2001**, *627*, 1090−1094.
(23) *WinXPow*, version 1.10; Stoe&Cie GmbH: Darmstadt, Germany, 2001.
(24) Sheldrick, G. M. *SHELX-97*; University Göttingen: Göttingen, Germany, 1997.

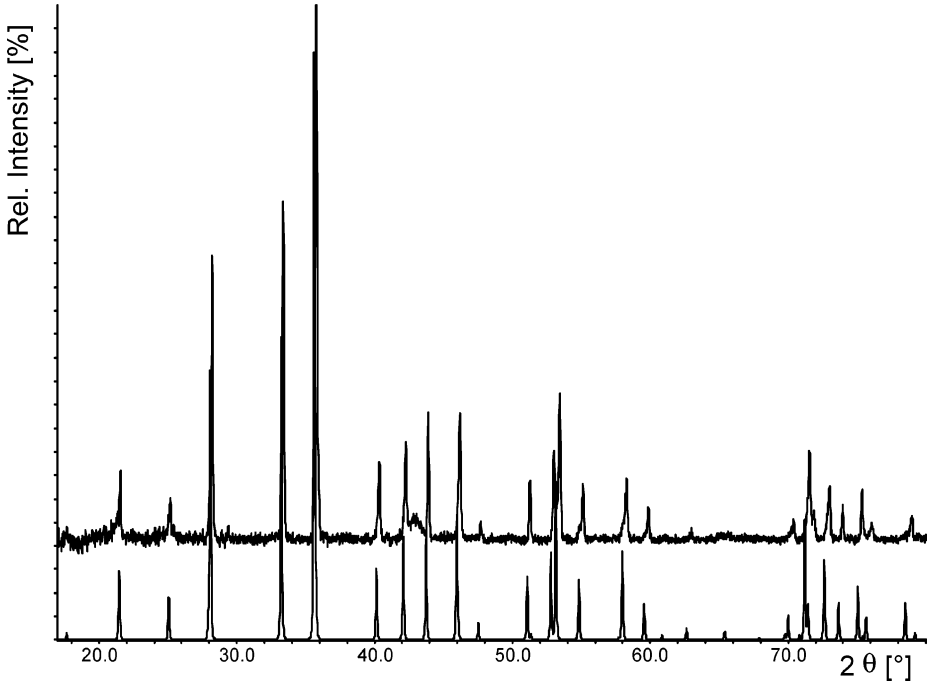

Figure 1. Comparison of the recorded (above) and calculated (below) X-ray powder patterns of $CaB_{4-x}C_x$. The peak at $2\theta = 43°$ is due to the sample preparation.

Table 1. Crystal Data and Parameters for Data Collection and Structure Refinement for CaB_4

sum formula, units per unit cell	CaB_4, 4
fw/(g/mol)	83.32
temp/K	293(2)
radiation, wavelength/Å, monochromator	Mo Kα, 0.71073, graphite
space group	*P*4/*mbm* (No. 127)
cell dimensions/Å	$a = 7.0989(7)$ $c = 4.1353(5)$
cell volume/Å^3	208.40(4)
calcd density/(g/cm^3)	2.656
abs coeff (mm^{-1})	2.53
measured range/deg	$10 \le 2\Theta \le 65$
index ranges	$-10 \le h \le 10$, $-10 \le k \le 10$, $-6 \le l \le 6$
observed reflns	2298
independent reflns	240 ($R_{int} = 0.034$)
R_1, wR_2 [$I > 2\sigma(I)$][a]	0.0231, 0.0571
residual electron density/ (10^{-6} *e* pm^{-3})	0.50 and −0.35

[a] $R_1 = (\sum_{hkl}||F_o| - |F_c||)/\sum_{hkl}|F_o|$; $wR_2 = \sqrt{\sum_{hkl} w(F_o^2 - F_c^2)^2/\sum_{hkl} w(F_o^2)^2}$.

Table 2. Atomic Coordinates and Isotropic Displacement Parameters in CaB_4

atom	position	*x*/*a*	*y*/*b*	*z*/*c*	U_{iso} (pm^2)
Ca	4g	0.31884(4)	0.818 84(4)	0	122(2)
B(1)	8j	0.1780(2)	0.0353(2)	1/2	107(5)
B(2)	4h	0.4168(2)	0.0831(2)	1/2	117(7)
B(3)	4e	0	0	0.2052(5)	112(7)

it showed only very small amounts (<1%) of carbon in the boron network, according to (WDS-EPMA) analyses.[25] To learn more about the role of carbon in $CaB_{4-x}C_x$, more experiments such as electron energy loss spectroscopy (EELS), inductively coupled plasma−atomic emission spectrometry (ICP−AES), and solid-state NMR were carried out.

(25) Garland, M. T.; Wiff, J. P.; Bauer, J.; Guérin, R.; Saillard, J.-Y. *Solid State Sci.* **2003**, *5*, 705−710.

Table 3. Anisotropic Displacement Parameters (pm^2) in CaB_4

atom	position	U_{11}	U_{22}	U_{33}	U_{23}	U_{13}	U_{12}
Ca	4g	118(2)	118(2)	130(2)	0	0	18(1)
B(1)	8j	118(8)	117(8)	85(7)	0	0	−3(5)
B(2)	4h	119(8)	119(8)	113(10)	0	0	−10(7)
B(3)	4e	123(8)	123(8)	89(9)	0	0	0

Table 4. Selected Interatomic Distances (in Å) in the Crystal Structure of CaB_4

B(1)−B(1)	1.822(2)	2×	B_6 octahedra
B(3)−B(1)	1.773(2)	4×	
B(2)−B(2)	1.670(5)	1×	B_2 dumbbell
B(3)−B(3)	1.697(4)	1×	connection octahedra−octahedra
B(1)−B(2)	1.729(2)	2×	connection octahedra−dumbbell
Ca−B	2.738(1)−3.142(2)	16×	CaB_{16} polyhedra

EELS. From the EEL spectrum (Gatan PEELS666 spectrometer), characteristic energy losses were found for Ca, B, and C. Although reliable quantitative elemental analyses from EEL spectra are only possible with suitable reference materials, a small amount of carbon was estimated from the EELS data, besides Ca and B (Figure 2).

ICP−AES. Quantitative analyses of the carbon content were performed by means of ICP−AES (LECO CS-444LS) measurements. $CaB_{4-x}C_x$ samples used for the analyses were prepared in two different batches, using Ca and B_4C as starting materials. Both products occurred as single-phase materials, according to their powder XRD pattern. For each experiment, a 5 mg sample was solubilized with 0.5 mg of Na_2CO_3 and 0.2 g of KNO_3. This mixture was dissolved in 2 mL of HNO_3 and then diluted for the ICP−AES measurement. The total carbon content was refined as 3.0 and 3.8 wt % from two different samples of $CaB_{4-x}C_x$. This corresponds to $CaB_{4-x}C_x$ with $x = 0.21$ and 0.26, respectively.

NMR. Solid-state ^{11}B and ^{13}C magic angle spinning (MAS) NMR experiments on $CaB_{4-x}C_x$ were carried out at 4.7 T (Bruker DSX 200, 4 mm o.d. zirconia rotors; ^{11}B, 64.21 MHz; ^{13}C, 50.32 MHz) and 11.75 T (Bruker Avance 500, 2.5 mm o.d. zirconia rotors; ^{11}B, 160.51 MHz; ^{13}C, 125.80 MHz). Chemical shifts are reported for ^{11}B with respect to $F_3B{\cdot}OEt_2$ using $NaBH_4$ (−42.06 ppm) as

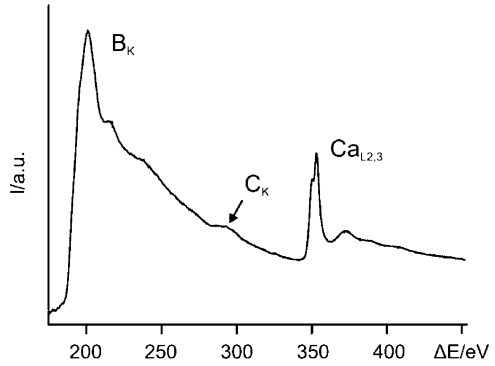

Figure 2. Electron energy loss spectrum showing the $Ca_{L2,3}$, B_K, and C_K edges.

an external secondary reference and for ^{13}C with respect to tetramethylsilane using adamantane (38.55 ppm, CH) as an external secondary reference. Samples for ^{13}C measurements were prepared with calcium, boron, and 100% ^{13}C as starting materials.

For comparison with $CaB_{4-x}C_x$, we also obtained the ^{11}B MAS NMR spectrum of a separately prepared sample of LaB_4 (Figure 3). The ^{11}B MAS NMR spectrum of LaB_4 shows two isotropic peaks at 39 and 12 ppm in a 1:1 ratio for the central transitions. However, a closer examination of the spinning sideband pattern associated with the ^{11}B satellite transitions reveals that the sideband manifold at higher frequencies actually consists of two equally populated sites with significantly different nuclear quadrupolar coupling constants. Analysis[26] of the satellite transitions yields nuclear quadrupolar coupling constants, $\chi = e^2qQ/h$, and asymmetry parameters of the electric field gradient tensor, $\eta = (q_{XX} - q_{YY})/q_{ZZ}$,[27] that are in excellent agreement with those reported by Creyghton et al.[28] for a static powder sample of LaB_4 at 4.2 K. Because of the limited resolution of ^{11}B static powder spectra, Creyghton et al. were not able to determine the different chemical shifts of the boron sites. In the present study, we obtained the following data (with chemical shifts corrected for second-order quadrupolar shifts): $\delta_{iso} = 42$ ppm, $\chi = 0.69$ MHz, $\eta = 0.00$ (site 4e); $\delta_{iso} = 47$ ppm, $\chi = 1.1$ MHz, $\eta = 0.05$ (site 4h); $\delta_{iso} = 18$ ppm, $\chi = 0.8$ MHz, $\eta = 0.5$ (site 8j).

Similar to LaB_4, the ^{11}B MAS NMR spectrum of $CaB_{4-x}C_x$ features two different isotropic peaks at 56 and 5 ppm for the central transitions, but the intensity ratio is 0.8:1. Again, the peak at 5 ppm is assigned to site 8j, with $\delta_{iso} = 11$ ppm, $\chi = 0.8$ MHz, and $\eta = 0.3$ (Figure 3). The spinning sidebands associated with the satellite transitions of 4e and 4h are very broad and, thus, much weaker in intensity. This finding suggests that a distribution rather than a unique set of quadrupolar parameters contributes to their appearance, possibly caused by disorder of the incorporated carbon atoms. Disorder is also the likely reason for the observed field dependence of the line width of the peak at 136 ppm in the ^{13}C MAS NMR spectrum of ^{13}C-enriched $CaB_{4-x}C_x$ (Figure 4), that is, 1300 Hz at 4.7 T and 2800 Hz at 11.75 T.

Magnetic Studies. The magnetic susceptibility behavior of $CaB_{4-x}C_x$ was studied with a SQUID magnetometer (Quantum Design, MPMS) in the temperature region between 20 and 300 K using a static field ($H = 1000$ G). The measurements revealed a temperature-independent paramagnetic behavior with a susceptibility on the order of $\chi_{mol} = 1 \times 10^{-3}$ cm^3/mol.

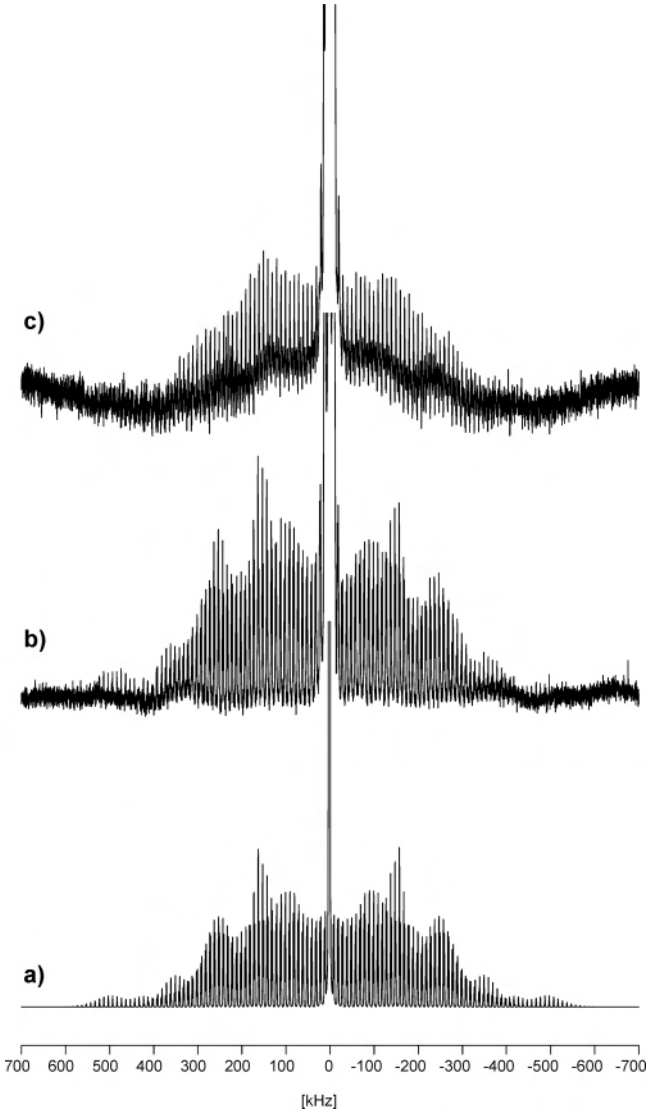

Figure 3. ^{11}B MAS NMR spectra obtained at 4.7 T for LaB_4, simulated using the parameters given in the text (a) and observed (b), and for $CaB_{4-x}C_x$ (c). Spinning rate: 10 kHz. The central transitions were cut off at 10% intensity.

Electronic Properties. The bonding properties and the electronic situation in $CaB_{4-x}C_x$ were investigated by extended Hückel calculations (YAeHMOP[29]) of the band structure on the basis of the refined crystal structure data of $CaB_{4-x}C_x$. Calculations were first performed under the assumption of a pure boride network containing four formula units of CaB_4 in the unit cell and cyclic boundary conditions. Changes in the electronic structure resulting from substitutions of boron atoms versus carbon atoms in the structure were studied afterward. Band structure calculations within the tetragonal primitive Brillouin zone were performed at 20 k points along each symmetry line connecting the special points $\Gamma = (0,0,0)$, $X = (0,^1/_2,0)$, $M = (^1/_2,^1/_2,0)$, $A = (^1/_2,^1/_2,^1/_2)$, $Z = (0,0,^1/_2)$, and $R = (0,^1/_2,^1/_2)$.[30] A set of 288 k points in the first reduced Brillouin zone was used for calculations of the average properties (density of states, DOS, and crystal orbital overlap population, COOP). The parameters employed in the calculations were adopted from the literature.[29]

(26) Eichele, K. *Csolids*, version 1.4.26; University of Tübingen: Tübingen, Germany, 2005.
(27) Abragam, A. *Principles of Nuclear Magnetism*; Clarendon Press: Oxford, U. K., 1961.
(28) Creyghton, J. H. N.; Locher, P. R.; Buschow, K. H. J. *Phys. Rev B* **1973**, *7*, 4829−4843.
(29) YAeHMOP, extended Hückel molecular orbital package, freely available on the Web at http://sourceforge.net/projects/yaehmop.
(30) Bradley, C. J.; Cracknell, A. P. *The Mathematical Theory of Symmetry in Solids*; Claredon Press: Oxford, U. K., 1972; pp 82−109.

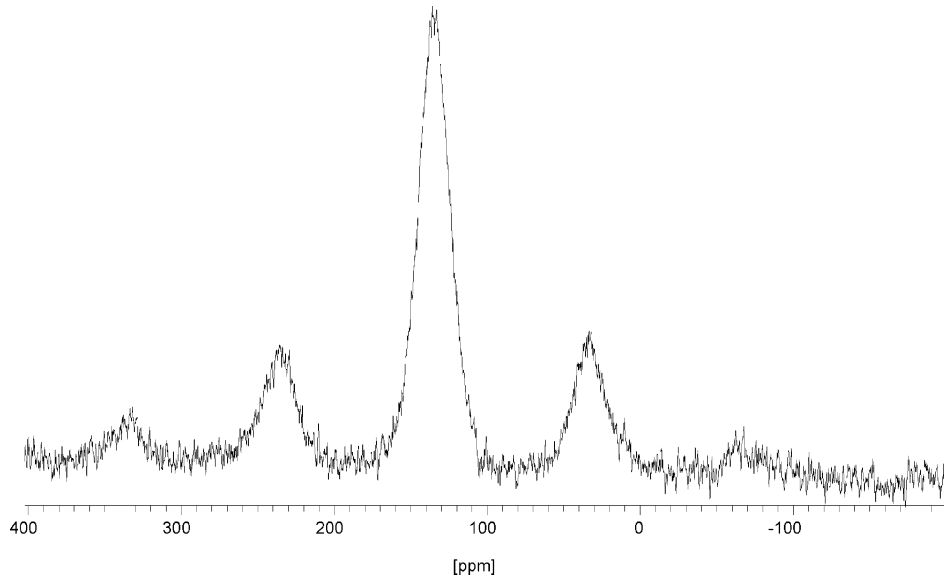

Figure 4. ^{13}C MAS NMR spectrum of $CaB_{4-x}C_x$ obtained at 4.7 T and with a spinning of 10 kHz.

Results and Discussion

Structure. The single-crystal structure refinement of $CaB_{4-x}C_x$ revealed a ThB_4-type structure that is well-known for many rare earth tetraborides. Boron atoms in this structure occupy three distinct special positions: B(1) occupies an 8j position and forms squares, B(2) occupies a 4h position and forms dumbbells, and B(3) is on a 4e position bicapping the squares to complete tetragonal B_6 bipyramides. Because the carbon content in $CaB_{4-x}C_x$ is relatively low, and may be expressed as $CaB_{3.8}C_{0.2}$ according to chemical analyses, the crystal structure is discussed simply as calcium tetraboride, which should, in fact, exist, as will be explained later.

The crystal structure of CaB_4 contains a boron network of slightly (D_{4h}) distorted B_6 octahedra [d_{B-B} = 1.822(2) Å (2×) and 1.773(2) Å (4×)] and ethylene-like B_2 dumbbells [d_{B-B} = 1.670(5) Å], which are combined into a three-dimensional network. A projection on the *ab* plane of the structure shows the connectivity of distorted boron octahedra and dumbbells forming a two-dimensional layer, displayed in Figure 5. The B−B bond lengths between octahedra and dumbbells are 1.729(2) Å. The seven-membered rings in this structure pattern are capped with Ca ions from above and below, with Ca ions being situated in a 16-fold environment [d_{Ca-B} = 2.738(1)−3.142(2) Å] of boron atoms. A view along the *c*-axis direction shows the apical connectivity of distorted B_6 octahedra (Figure 6) with B−B bond lengths of 1.697(4) Å.

Electronic Considerations. The electronic requirement of the boron network in MB_6 hexaborides is generally considered to be $[B_6]^{2-}$, similar to that in the molecular $[B_6H_6]^{2-}$ species. Consequently, hexaborides with divalent cations occur as $M^{2+}[B_6]^{2-}$ semiconductors, whereas those with trivalent cations may be considered as $M^{3+}[B_6]^{2-}\cdot(e^-)$ metals, because of one excess electron per formula unit. The electronic situation of tetraborides with the ThB_4-type structure has been proposed by Lipscomb and Britton.[31] Following this concept, the MB_4 structure is first decomposed into fragments of closo-B_6 clusters and ethylene-like B_2 units. A closo-B_6 cluster requires ($4n + 2$) 14 electrons, and the ethylene-like B_2 unit requires four electrons. When these fragments are being linked via B−B single bonds, six additional electrons for each B_6 cluster and four additional electrons for each ethylene-like B_2 unit are required. When the unit cell content ($Z = 4$) of M_4B_{16} or $M_4(B_6)_2(B_2)_2$ is considered with two B_6 octahedra and two B_2 dumbbells, 56 electrons are required for the stabilization of the boron network. This exactly matches the number of valence electrons in Ca_4B_{16}. It can be, therefore, assumed that tetraborides possessing the ThB_4-type structure occur as stable compounds with a divalent cation.

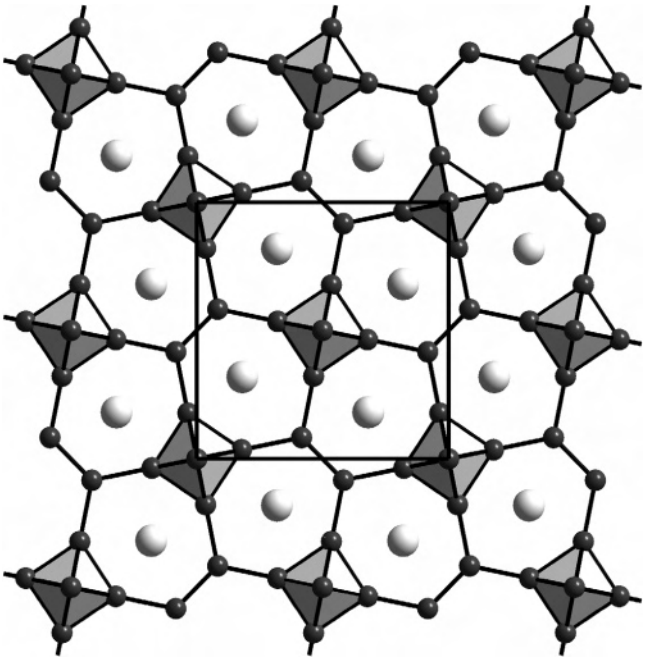

Figure 5. Connectivity of B_6 octahedra and B_2 dumbbells in the *ab* plane in the crystal structure of CaB_4. Ca is shown gray and B black.

(31) Lipscomb, W. N.; Britton, D. *J. Chem. Phys.* **1960**, *33*, 275−280.

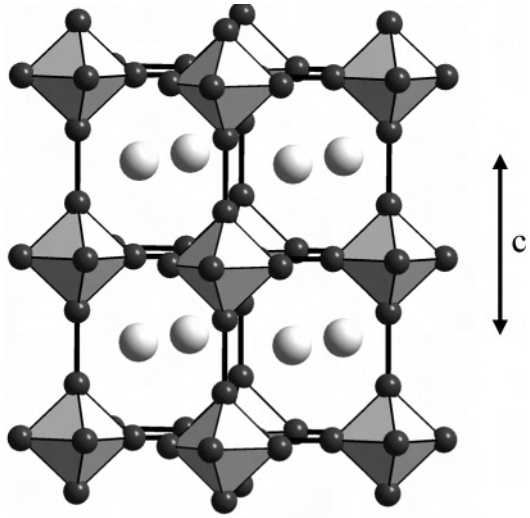

Figure 6. Connectivity of the B_6 octahedra along the *c*-axis direction in the crystal structure of CaB_4.

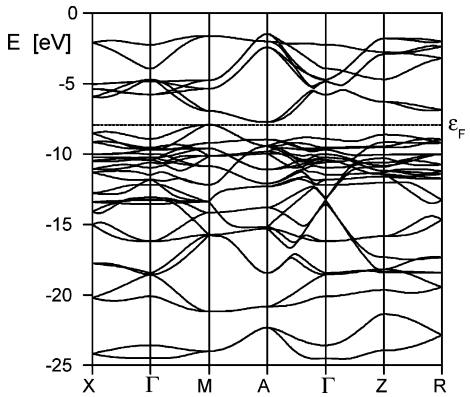

Figure 7. Calculated band structure of CaB_4 along several special points of the first Brillouin zone for a primitive tetragonal lattice.

Electronic Properties. The band structure of CaB_4 was calculated along several directions of the reciprocal space and is displayed in Figure 7. The calculations revealed a very small indirect band gap on the order of 0.2 eV above the Fermi level (ϵ_F, shown as dotted line). All of the energy bands in the depicted area are dominated by orbital contributions from boron atoms. Orbital contributions of Ca play only a minor role in the region around the Fermi level because their empty 4s orbitals are at higher energies. Ca as a divalent cation hardly takes part in covalent interactions with the boron network. This behavior is in clear contrast to the electronic structure of GdB_4, where the d orbitals of Gd interact with orbitals of the boron network, as we will describe later.[25]

An analysis of the energy bands shows varying orbital contributions of the constituting fragments (B_6 octahedra and B_2 dumbbells) of the boron network. In Figure 8, the total DOS and the respective contribution of the B_6 octahedra are shown. In the area slightly above the Fermi level, a relatively low contribution of B_6 states can be seen. A further analysis of the COOPs shows transitions from B−B bonding interactions below the Fermi level to B−B antibonding interactions above, for both fragments (Figure 9). In particular, the transition from strong bonding to strong antibonding within

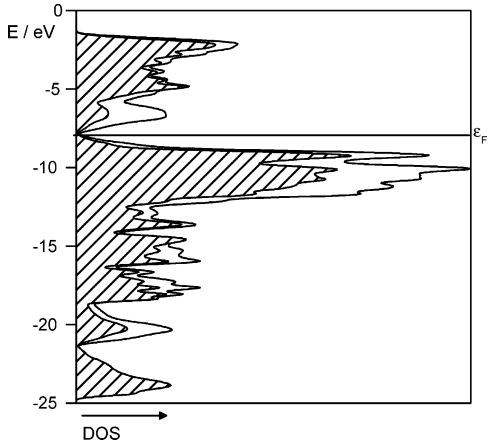

Figure 8. Calculated total DOS of CaB_4. The DOS contribution of B_6 octahedra to the total DOS is shown as a lined area.

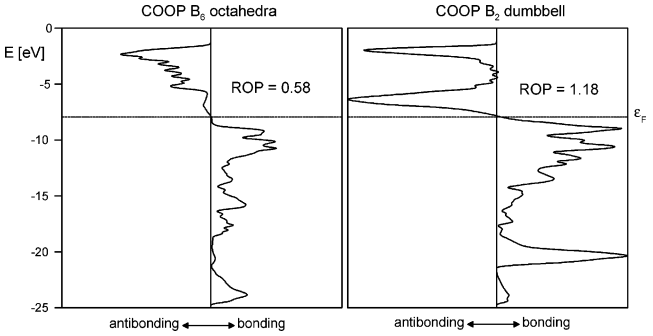

Figure 9. COOPs for B_6 octahedra (left) and B_2 dumbbells (right) in the structure of CaB_4.

the B_2 unit is remarkable. A closer examination of the crystal orbitals of the B_2 unit reveals strong bonding π interactions up to the Fermi level (indicating a B−B double bond) and strong antibonding π^* interactions above ϵ_F. A Mulliken analysis carried out for both fragments leads to reduced overlap populations of 0.58 for the B_6 octahedra and 1.18 for the B_2 dumbbell up to ϵ_F. This finding supports the assumption of ethylene-like $[B_2]^{2-}$ units and $[B_6]^{2-}$ octahedra, which are interconnected with each other via B−B single bonds into a three-dimensional boron network. A simplified charge picture can be postulated as $(Ca^{2+})_2[B_6]^{2-}[B_2]^{2-}$. The results of our extended Hückel calculations fully confirm the closed-shell assumption proposed by Lipscomb and Britton, which requires a divalent cation for the stabilization of the boron network in ThB_4-type structures.

In the next step, calculations were performed on structural models in which boron atoms were partially substituted by carbon atoms, first on one and then on all three distinct positions. Because of the increased number of electrons, the Fermi level went up to higher energy, leading to occupations of antibonding orbitals in the boron/carbon network. In any case, the largest impact on bonding properties was found for the B_2 unit, where the partial occupations of π^* orbitals caused a weakening of B−B bonding, for example, with a reduction in the overlap populations down to 0.80 for $CaB_{3,75}C_{0,25}$.

The bonding in the B_2 unit in the structure of GdB_4 is weakened through electron donations of B−B π bonding into Gd d orbitals. Despite the sp^2 hybridization of each B atom

in the B_2 unit, there is, rather, a B−B single bond to be considered between atoms of the dumbbell.[25] A comparison of the B−B bond lengths in CaB_4 and those of the rare earth tetraborides supports this assumption. For CaB_4, the B−B distance in the B_2 dumbbell is 1.670(5) Å, whereas in the rare earth tetraborides MB_4 (M = Y, La, Ce, Nd, Sm, Gd, Tb, Dy, and Er), the average distance in the B_2 dumbbell increases by about 8 pm to 1.752 Å. All of the other B−B bonding interactions in CaB_4 show only minor deviations from average values found for the rare earth tetraborides.

From the calculated band gap of 0.2 eV, we assume semiconducting behavior for CaB_4. Carbon-doped $CaB_{4-x}C_x$ is, however, expected to behave as metallic. This is in agreement with both the obtained metallic luster and the temperature-independent paramagnetic behavior of $\chi_{mol} = 1 \times 10^{-3}$ cm^3/mol in the temperature range between 20 and 300 K. Measurements of the electrical conductivity are not available because of intrinsic adhesion problems between crystals and several fluid contact media.

Conclusion

The existence of isotypic structures for CaB_6 and LaB_6 and their distinct properties as semiconducting and metallic materials are well-known. The electronic requirement of an isolated network of boron octahedra as present in these structures is considered to be $[B_6]^{2-}$. The crystal structure of lanthanide tetraborides, such as LaB_4, contains a network structure composed of boron octahedra and boron dumbbells ($La_2[B_6](B_2]$). The existence of a corresponding CaB_4 counterpart of LaB_4 has remained unknown until now.

The structure of the carbon-doped calcium tetraboride is isotypic with the structure of LaB_4. The carbon content of $CaB_{4-x}C_x$ is rather low (<5%), but the presence of carbon turned out to be essential for the synthesis of this compound.

Upon first glance, it could be assumed that carbon may have a stabilizing effect by achieving the same valence electron number ("CaB_3C") as that for LaB_4. This simple consideration does not, however, satisfy the distinct bonding requirements with cations in both types of compounds. Theoretical considerations and band structure calculations have demonstrated that CaB_4 can be regarded as an electronically stable compound, eventually even more stable than carbon-doped calcium tetraboride. The electronic charge picture of CaB_4 with the constituting B_6 octahedra and B_2 dumbbells is approximated as $(Ca^{2+})_2[B_6]^{2-}[B_2]^{2-}$. The ethylene-like B_2 dumbbell displays clear characteristics of B−B double-bonding interactions in CaB_4, although this type of bonding is not well-established in boron chemistry. Moving to the corresponding lanthanide tetraborides, we note differences in the bonding behavior of the dumbbells. Here, the π orbitals of the dumbbells overlap with the d orbitals of the lanthanide ions, and a pronounced increase of the electrical conductivity can be regarded from the electron delocalization over these orbitals. This finding is consistent with the 8-pm-shorter B−B distance in the dumbbell of CaB_4. We note a similar interaction for lanthanide dicarbides, for example, in LaC_2. In this case, interactions between the (C−C antibonding) π^* orbitals of dicarbide dumbbells and the La d orbitals also relate to an 8-pm-shorter C−C distance in the isotypic CaC_2.

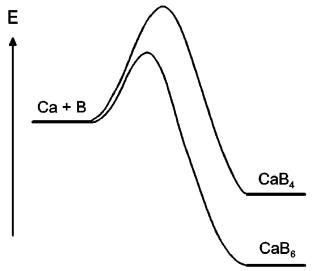

Figure 10. Hypothetical activation barriers and relative stabilities of CaB_4 and CaB_6.

Although the role of carbon in the reaction is to date not well understood, one hypothesis could be that the formation of pure calcium tetraboride from calcium and boron is hindered kinetically as well as thermodynamically (Figure 10). The presence of carbon in the reaction and the formation of CaC_2 and CaB_2C_2 as intermediates may allow a moderate reaction pathway to yield a carbon-doped CaB_4 that decomposes into (thermodynamically stable) CaB_6 at elevated temperatures (≥1000 °C). In this context, it may be worthwhile to note that the formation of higher borides is also a problem in the synthesis of MgB_2, resulting from the evaporation of Mg metal at elevated temperatures.

Acknowledgment. The authors express their thanks to Dr. K. Hofmann and Prof. B. Albert (Universität Hamburg, Germany) for their valuable support with EELS measurements. We are very grateful to Prof. T. Mori (National Institute for Materials Science, Tsukuba, Japan) for generous help with ICP-AES analyses. Prof. R. E. Wasylishen (University of Alberta, Canada) is acknowledged for instrument time on the Avance 500. R.S. gratefully acknowledges a fellowship from the Studienstiftung des Deutschen Volkes.

Supporting Information Available: Additional tables and crystallographic data in cif format. This material is available free of charge via the Internet at http://pubs.acs.org.

IC0518430